ASTRONOMY & ASTROPHYSICS
SUPPLEMENT SERIES

Astron. Astrophys. Suppl. Ser. **137**, 157–163 (1999)

Recombination coefficients for the 5g − 4f transitions of O III at nebular temperatures and densities⋆

R. Kisielius and P.J. Storey

Department of Physics and Astronomy, University College London, Gower Street, London WC1E 6BT, UK

Received February 1; accepted February 22, 1999

Abstract. We calculate effective recombination coefficients for the formation of the 5g − 4f lines of O III in the intermediate coupling scheme. Photoionization data for the 5g levels calculated using the R-matrix method are used to derive their recombination coefficients. Cascading from higher states is included, allowing for the effects of finite electron density in a hydrogenic approximation. We explicitly include the distribution of population between the two ground levels of O^{3+} in the calculation of the line intensities. The results are presented as a simple programmeable formula allowing the calculation of recombination line intensities for electron temperatures, T_e in the range 5000 − 20 000 K and electron densities, N_e in the range $10^2 - 10^6$ cm^{-3}.

Key words: atomic data — atomic processes — line: formation — ISM: H II regions — ISM: planetary nebulae: general

1. Introduction

Increasing use is being made of weak recombination lines to determine elemental abundances in photoionized nebulae relative to hydrogen (e.g. Liu et al. 1995). The most prominent lines of C, N, O and Ne arise from once ionized species for which reliable theoretical recombination coefficients are becoming available. Péquignot et al. (1991) have computed coefficients for selected lines of C, N and O in a relatively simple approximation, while more comprehensive and accurate calcaulations have been made by Davey et al. (1999) for C II, by Escalante & Victor (1990) for N II, by Storey (1994) for O II and by Kisielius et al. (1998) for Ne II. For these once ionized species the transition arrays 4f − 3d, 3d − 3p and 3p − 3s fall in the blue part of the spectrum, mainly between 3500 and 5000 Å and are readily accessible to large ground-based telescopes. For twice ionized species, these transition arrays fall in the ultraviolet and are not easily observed, but the 5g − 4f transition arrays once again fall in the blue. In O^{2+}, the 5g − 4f transitions lie between 4300 Å and 4600 Å and can be used to determine the O^{3+} abundance.

Péquignot & Baluteau (1994) have recently identified forbidden lines from elements with $Z > 30$ in very deep red spectra of the planetary nebula NGC 7027. To be confident of the measured intensities of such lines it is necessary to understand the weak recombination lines, such as those of the 5g − 4f array, that are also present in the spectra with comparable intensity.

2. Atomic data for O^{2+}

In Table 1 we present experimental and calculated level energies for the two electron configurations $1s^22s^22p4f$ and $1s^22s^22p5g$. The experimental values are from Pettersson (1982), with the energies being given relative to the lowest levels of the 4f configuration in each case. Two different methods were used to obtain the theoretical results.

In the first approach, we used the general purpose atomic structure package SUPERSTRUCTURE (SS, Eissner et al. 1974; Nussbaumer & Storey 1978) to calculate wavefunctions for O^{2+}. Only the $1s^22s^22p4f$ and $1s^22s^22p5g$ electron configurations were included in the calculation. The scaled Thomas-Fermi-Dirac potentials for the common radial basis functions were varied to minimize the sum of the energies of all twelve terms. The non-relativistic Hamiltonian matrix was adjusted empirically to give the best possible agreement between calculated term energies (obtained from the weighted mean of the fine-structure energies) and the experimental values. The 4f and 5g spin-orbit parameters were also adjusted empirically to give the best agreement between the calculated and experimental fine-structure level

Send offprint requests to: P.J. Storey

⋆ All tables are available in electronic form at the CDS via anonymous ftp to cdsarc.u-strasbg.fr (130.79.128.5) or via http://cdsweb.u-strasbg.fr/Abstract.html

Table 1. Indices (n_1) and energy levels (in cm^{-1}) of the 4f and 5g states in O^{2+} ions. Experimental energy data are from Pettersson (1982) while theoretical values are from SUPERSTRUCTURE (SS) and an R-matrix (RM) calculation. We also give our theoretical (SS) and previous experimental (Moore 1970) level assignments

		Level		Energy		
n_1	Configuration	SS	Exp	Exp	SS	RM
1	$(^2P^o_{1/2})4f$	$^3F_3$	$F[2\frac{1}{2}]_3$	0.0	0.0	0.0
2	$(^2P^o_{1/2})4f$	$^3F_2$	$F[2\frac{1}{2}]_2$	13.5	12.6	13.2
3	$(^2P^o_{1/2})4f$	$^1F_3$	$F[3\frac{1}{2}]_3$	59.1	58.7	55.5
4	$(^2P^o_{1/2})4f$	$^3F_4$	$F[3\frac{1}{2}]_4$	75.1	74.5	72.2
5	$(^2P^o_{3/2})4f$	$^3G_3$	$G[3\frac{1}{2}]_3$	567.1	566.0	548.0
6	$(^2P^o_{3/2})4f$	$^3G_4$	$G[3\frac{1}{2}]_4$	600.9	600.0	581.8
7	$(^2P^o_{3/2})4f$	$^3G_5$	$G[4\frac{1}{2}]_5$	793.9	794.6	773.6
8	$(^2P^o_{3/2})4f$	$^3D_3$	$D[2\frac{1}{2}]_3$	844.7	844.1	855.4
9	$(^2P^o_{3/2})4f$	$^1G_4$	$G[4\frac{1}{2}]_4$	862.6	863.3	895.4
10	$(^2P^o_{3/2})4f$	$^3D_2$	$D[2\frac{1}{2}]_2$	867.5	867.3	885.4
11	$(^2P^o_{3/2})4f$	$^3D_1$	$D[1\frac{1}{2}]_1$	1013.6	1013.6	1023.1
12	$(^2P^o_{3/2})4f$	$^1D_2$	$D[1\frac{1}{2}]_2$	1034.4	1035.3	1055.2
13	$(^2P^o_{1/2})5g$	$^1G_4$	$G[3\frac{1}{2}]_4$	22892.6	22892.8	22539.4
14	$(^2P^o_{1/2})5g$	$^3G_3$	$G[3\frac{1}{2}]_3$	22892.6	22892.9	22539.6
15	$(^2P^o_{1/2})5g$	$^3H_4$	$G[4\frac{1}{2}]_4$	22901.8	22900.2	22547.9
16	$(^2P^o_{1/2})5g$	$^3H_5$	$G[4\frac{1}{2}]_5$	22901.8	22900.7	22548.6
17	$(^2P^o_{3/2})5g$	$^3G_4$	$H[4\frac{1}{2}]_4$	23245.3	23248.2	22890.5
18	$(^2P^o_{3/2})5g$	$^3G_5$	$H[4\frac{1}{2}]_5$	23245.3	23248.7	22891.2
19	$(^2P^o_{3/2})5g$	$^3F_4$	$H[5\frac{1}{2}]_4$	23290.0	23292.7	22940.3
20	$(^2P^o_{3/2})5g$	$^3F_3$	$H[5\frac{1}{2}]_3$	23290.0	23292.9	22940.3
21	$(^2P^o_{3/2})5g$	$^3H_6$	$F[3\frac{1}{2}]_6$	23337.5	23338.2	22987.2
22	$(^2P^o_{3/2})5g$	$^1H_5$	$F[3\frac{1}{2}]_5$	23337.5	23338.7	22987.4
23	$(^2P^o_{3/2})5g$	$^3F_2$	$F[2\frac{1}{2}]_2$	23373.5	23375.0	23027.5
24	$(^2P^o_{3/2})5g$	$^1F_3$	$F[2\frac{1}{2}]_3$	23373.5	23375.4	23028.3

energies within the terms. This procedure was first implemented in SS by Zeippen et al. (1977). These empirical adjustments, although very small compared to the absolute energies of the levels, are important in obtaining accurate eigenvectors for levels of the same total angular momentum and parity ($J\pi$). It can be seen from Table 1 that the energy separations between such levels may be only a few tens of cm^{-1}. An error of a few wavenumbers in these energy separations can therefore cause significant errors in the eigenvectors, and since we cannot achieve this level of accuracy in our ab initio calculation, we make empirical corrections. The maximum difference in the energies between the empirically corrected SS calculation and experiment is 3.4 cm^{-1}, with an average of 1.2 cm^{-1}. In addition to the level assignments obtained from the SS calculation, we also provide level assignements from Moore (1970).

In our second theoretical approach, we use the R-matrix method (Berrington et al. 1987) in which bound-bound and bound-free radiative data for O^{2+} states are calculated from the O^{3+} + e$^-$ scattering problem. Some relativistic terms are included in the Hamiltonian in the Breit-Pauli approximation. One-body energy shifts (the mass correction and the Darwin term) and the spin-orbit interaction are incorporated within this implementation of the R-matrix method (Scott & Taylor 1982; Berrington et al. 1995).

The O^{3+} target system is represented by the two ground levels 2p $^2P^o_{1/2}$ and $^2P^o_{3/2}$, with the wave function basis consisting of the $2s^22p$ and $2p^3$ configurations and with the target radial waves being obtained from SS. The experimental fine-structure splitting was used for the two target levels before constructing the Hamiltonian for the $(N+1)$-electron system, to compensate for the absence of two-body fine-structure terms in the Hamiltonian. The target fine-structure energy calculated including only the spin-orbit terms is 379.1 cm^{-1} compared to the experimental value of 385.9 cm^{-1}. This empirical correction to the target energies is the only correction that can be made in the R-matrix approach. In particular no empirical corrections to the eigenvectors of the O^{2+} bound states can be made as was done in the SS calculation. As a result the accuracy of the calculated energies is significantly worse than in the SS calculation, with average differences of 13.1 cm^{-1} for the 4f levels and 2.7 cm^{-1} for the 5g levels (taken relative to the energetically lowest 5g level).

There is also a systematic shift of approximately 350 cm^{-1} between the levels of the 5g and 4f configurations compared to experiment.

In view of the significantly higher accuracy of the empirically corrected SS level energies, we used this method to calculate the radiative transition data. Transition matrix elements were computed and combined with experimental energy level data to obtain the final transition probabilities which are given in Table 2. Also given in this table are wavelengths $\lambda_{\rm air}$ and branching ratios from each upper state. It should be noted that the wavelengths presented in Table 2 are derived from the experimental energy level data (Pettersson 1982) and may differ slightly from the observed wavelengths. These data will be used later to produce synthetic emission spectra of the 5g − 4f recombination lines.

3. Recombination coefficients

We base our calculation of the recombination coefficients on a model of the O^{2+} ion including the two series $1s^22s^22p(^2P^o_{1/2})nl$ and $1s^22s^22p(^2P^o_{3/2})nl$. At low electron densities $N_{\rm e}$, the population of the ground levels $^2P^o_{1/2}$ and $^2P^o_{3/2}$ in the recombining ion O^{3+} differs significantly from the Boltzmann distribution. The critical density, defined as the electron density at which the rate of collisional de-excitation of $^2P^o_{3/2}$ is equal to the rate of radiative de-excitation, is 7330 cm^{-3} at a temperature of 10^4 K. Thus for typical nebular densities the relative populations of the levels of the two series $(^2P^o_{1/2})nl$ and $(^2P^o_{3/2})nl$ will depend on density (as well as temperature $T_{\rm e}$).

Table 2. Wavelengths in air $\lambda_{\rm air}$ (in Å), electric dipole transition probabilities A_{n_1,n_2} (in $\rm s^{-1}$) and branching ratios b_{n_1,n_2} for the 5g − 4f transitions in $\rm O^{2+}$ ions. The indices n_1 and n_2 correspond to the energy level indices in Table 1

n_1	n_2	$\lambda_{\rm air}$	A_{n_1,n_2}	b_{n_1,n_2}	n_1	n_2	$\lambda_{\rm air}$	A_{n_1,n_2}	b_{n_1,n_2}
13	1	4366.997	2.96(+8)	8.029(−1)	19	1	4292.481	4.50(+7)	1.244(−1)
13	3	4378.300	1.16(+7)	3.142(−2)	19	3	4303.401	1.07(+5)	2.970(−4)
13	4	4381.370	2.87(+6)	7.798(−3)	19	4	4306.367	2.66(+7)	7.362(−2)
13	5	4477.926	1.20(+5)	3.275(−4)	19	5	4399.611	6.67(+5)	1.845(−3)
13	6	4484.716	1.06(+7)	2.879(−2)	19	6	4406.165	2.09(+7)	5.775(−2)
13	7	4523.884	4.70(+4)	1.276(−4)	19	7	4443.967	9.86(+5)	2.727(−3)
13	8	4534.308	4.69(+7)	1.273(−1)	19	8	4454.026	2.67(+8)	7.370(−1)
13	9	4537.992	5.03(+5)	1.365(−3)	19	9	4457.580	8.52(+5)	2.357(−3)
14	1	4366.997	1.65(+7)	4.471(−2)	20	1	4292.481	2.24(+5)	6.207(−4)
14	2	4369.573	2.91(+8)	7.917(−1)	20	2	4294.970	4.28(+7)	1.187(−1)
14	3	4378.300	1.00(+6)	2.718(−3)	20	3	4303.401	2.72(+7)	7.532(−2)
14	4	4381.370	1.06(+5)	2.892(−4)	20	4	4306.367	9.37(+5)	2.596(−3)
14	5	4477.926	1.10(+7)	2.995(−2)	20	5	4399.611	2.25(+7)	6.241(−2)
14	6	4484.716	4.45(+5)	1.209(−3)	20	6	4406.165	1.17(+6)	3.242(−3)
14	8	4534.308	2.22(+6)	6.034(−3)	20	8	4454.026	1.31(+7)	3.625(−2)
14	9	4537.992	7.72(+3)	2.099(−5)	20	9	4457.580	6.90(+5)	1.913(−3)
14	10	4539.002	4.45(+7)	1.209(−1)	20	10	4458.555	2.48(+8)	6.881(−1)
14	12	4573.660	9.11(+5)	2.477(−3)	20	12	4491.991	3.93(+6)	1.090(−2)
15	1	4365.242	8.21(+6)	2.239(−2)	21	7	4434.604	3.58(+8)	1.000(+0)
15	3	4376.536	2.66(+8)	7.260(−1)	22	4	4297.574	2.26(+5)	6.347(−4)
15	4	4379.604	7.45(+6)	2.031(−2)	22	6	4396.960	1.29(+7)	3.619(−2)
15	5	4476.082	8.15(+7)	2.221(−1)	22	7	4434.604	6.39(+6)	1.797(−2)
15	6	4482.866	1.75(+6)	4.774(−3)	22	9	4448.159	3.36(+8)	9.452(−1)
15	7	4522.002	2.02(+4)	5.515(−5)	23	1	4277.146	7.97(+5)	2.259(−3)
15	8	4532.417	1.25(+3)	3.400(−6)	23	2	4279.618	1.64(+7)	4.650(−2)
15	9	4536.098	1.59(+6)	4.340(−3)	23	3	4287.988	1.16(+6)	3.286(−3)
16	4	4379.604	2.76(+8)	7.545(−1)	23	5	4383.502	1.14(+6)	3.235(−3)
16	6	4482.866	8.48(+7)	2.321(−1)	23	8	4437.517	2.25(+6)	6.380(−3)
16	7	4522.002	8.74(+5)	2.393(−3)	23	10	4442.013	3.91(+7)	1.107(−1)
16	9	4536.098	4.00(+6)	1.095(−2)	23	11	4471.037	2.70(+8)	7.647(−1)
17	1	4300.735	3.10(+6)	8.400(−3)	23	12	4475.200	2.22(+7)	6.286(−2)
17	3	4311.698	7.64(+7)	2.070(−1)	24	1	4277.146	1.65(+7)	4.692(−2)
17	4	4314.675	2.05(+6)	5.550(−3)	24	2	4279.618	1.07(+6)	3.029(−3)
17	5	4408.283	2.52(+8)	6.818(−1)	24	3	4287.988	3.00(+5)	8.511(−4)
17	6	4414.863	1.32(+7)	3.588(−2)	24	4	4290.933	8.06(+5)	2.292(−3)
17	7	4452.815	6.35(+5)	1.720(−3)	24	5	4383.502	4.40(+4)	1.250(−4)
17	8	4462.914	5.90(+3)	1.600(−5)	24	6	4390.009	1.02(+6)	2.890(−3)
17	9	4466.483	2.20(+7)	5.962(−2)	24	8	4437.517	3.17(+7)	9.009(−2)
18	4	4314.675	8.74(+7)	2.376(−1)	24	9	4441.046	3.22(+4)	9.145(−5)
18	6	4414.863	2.40(+8)	6.537(−1)	24	10	4442.013	1.01(+6)	2.865(−3)
18	7	4452.815	2.82(+7)	7.657(−2)	24	12	4475.200	2.99(+8)	8.509(−1)
18	9	4466.483	1.18(+7)	3.214(−2)					

To calculate recombination coefficients $\alpha(5{\rm g}\,J\pi)$ and effective recombination coefficients for the lines originating from the 5g $(J\pi)$ levels, we consider the contribution to the 5g level population made both by direct recombination from the two parent levels and by cascades within the same series and between the two series. For sufficiently high orbital angular momentum of the valence electron, jj-coupling prevails and the population of a given level depends only on the population of other levels with the same parent and on direct recombination from that parent state. The 4f and 5g levels lie at intermediate orbital angular momentum where neither LS- nor jj-coupling are good descriptions. We calculate the recombination coefficients to the 5g $(J\pi)$ levels from the expression

$$\begin{aligned}\alpha(5{\rm g}\,J\pi) = {} & \mathcal{N}_1\,\alpha_1^{\rm dir}(J\pi) + \mathcal{N}_2\,\alpha_2^{\rm dir}(J\pi) \\ & + \mathcal{N}_1\,g_1^{\rm casc}(J\pi)\;\alpha_{\rm H}^{\rm casc}(5{\rm g})\frac{2J+1}{\omega(5{\rm g})\;\omega\left(^2{\rm P}^{\rm o}_{1/2}\right)} \\ & + \mathcal{N}_2\,g_2^{\rm casc}(J\pi)\,\alpha_{\rm H}^{\rm casc}\;(5{\rm g})\frac{2J+1}{\omega(5{\rm g})\;\omega\left(^2{\rm P}^{\rm o}_{3/2}\right)}, \qquad (1)\end{aligned}$$

where the ω are statistical weights, with $\omega(^2{\rm P}^{\rm o}_{1/2}) = 2$, $\omega(^2{\rm P}^{\rm o}_{3/2}) = 4$ and $\omega(5{\rm g}) = 18$. $\mathcal{N}_1$ and $\mathcal{N}_2$ are the

fractions of the O^{3+} population in the $^2P^o_{1/2}$ and $^2P^o_{3/2}$ states respectively and $\mathcal{N}_1 + \mathcal{N}_2 = 1$.

In Eq. (1), the $\alpha_i^{\rm dir}(J\pi)$ $(i = 1, 2)$ are the direct radiative recombination coefficients to the 5g $(J\pi)$ level. These coefficients were computed from the appropriate photoionization cross-sections obtained from the R-matrix calculations performed in the Breit-Pauli approximation described in Sect. 2.

The third and fourth terms in Eq. (1) are the cascade contributions. The coefficients $\alpha_{\rm H}^{\rm casc}(5g)$ are the combined cascade contributions to all 5g levels calculated in a hydrogenic approximation. These coefficients were obtained using the methods described by Storey & Hummer (1995) and include full allowance for all radiative and collisional processes between excited states, and as a result depend upon both temperature and density. We assume that the fraction of the cascading represented by the coefficient $\alpha_{\rm H}^{\rm casc}(5g)$ that falls on a particular level 5g $(J\pi)$ is proportional to its statistical weight and also that there are cascade contributions from states of both parentage. The fraction from each parent is given by the coefficients $g_1^{\rm casc}(J\pi)$ and $g_2^{\rm casc}(J\pi)$, which are determined from the photoionization cross-sections from the state 5g $(J\pi)$ at the two parent thresholds.

3.1. Evaluation of the coefficients

The coefficients $\alpha(5g\,J\pi)$ in Eq. (1) can be computed as follows. We have fitted the coefficients $\alpha_i^{\rm dir}(J\pi)$ as a function of temperature by:

$$\alpha_i^{\rm dir}(J\pi) = 10^{-15} a_i\, t^{b_i} \left(1 + c_i t + d_i t^2\right) \quad [{\rm cm^3\ s^{-1}}], \qquad (2)$$

where $t = T\ [{\rm K}]/10^4$. The fitting coefficients a_i, b_i, c_i and d_i are presented in Table 3.

The cascade contributions, $\alpha_{\rm H}^{\rm casc}(5g)$, can be fitted with a maximum error of 2% by a product of a function of density and a function of temperature as follows:

$$\alpha_{\rm H}^{\rm casc}(5g) = 0.69808\ 10^{-12}\ t^{a_{\rm t}}\ \left(1 + b_{\rm t} t + c_{\rm t} t^2\right) \times \left(1 + a_{\rm d} Y + b_{\rm d} Y^2 + c_{\rm d} Y^3\right)\ [{\rm cm^3\ s^{-1}}], \qquad (3)$$

where $t = T_{\rm e}\ [{\rm K}]/10^4$ and $Y = \log(N_{\rm e}) - 2$. The values of the fitting parameters are, for the temperature dependence, $a_{\rm t} = -0.94619$, $b_{\rm t} = -0.20470$, $c_{\rm t} = 0.02837$, and for the density dependance, $a_{\rm d} = -0.0086442$, $b_{\rm d} = -0.0013913$, $c_{\rm d} = -0.0005993$. The fits given in Eq. (2) and Eq. (3) are valid for $5000 \le T_{\rm e}[{\rm K}] \le 20\,000$ and $10^2 \le N_{\rm e}[{\rm cm^{-3}}] \le 10^6$, and the fitting error is less than 0.03% in these ranges.

The fractional populations $\mathcal{N}_1$ and $\mathcal{N}_2$ can be expressed as follows:

$$\mathcal{N}_1 = \frac{1}{1+X} \qquad (4)$$

Table 3. Fitting coefficients for $\alpha_i^{\rm dir}(J\pi)$, the direct recombination to the 5g levels of O^{2+}

n_1	a_1	b_1	c_1	d_1
13	11.8009	−0.5620	−0.2070	0.0255
14	9.1260	−0.5640	−0.2020	0.0241
15	13.1900	−0.5469	−0.2135	0.0266
16	16.0049	−0.5518	−0.2059	0.0245
17	1.0613	−1.3123	0.1673	−0.0245
18	1.3070	−1.3069	0.1578	−0.0231
19	1.2819	−1.2250	0.1855	−0.0311
20	1.0075	−1.2138	0.1904	−0.0315
21	1.5039	−1.3207	0.1283	−0.0176
22	1.2806	−1.3284	0.1386	−0.0197
23	0.4670	−1.4083	−0.0680	0.0117
24	0.7113	−1.4063	−0.0680	0.0121
	a_2	b_2	c_2	d_2
13	1.0104	−0.5473	−0.2022	0.0235
14	0.7891	−0.5456	−0.2064	0.0248
15	0.2551	−0.5411	−0.2139	0.0270
16	0.3136	−0.5413	−0.2127	0.0264
17	6.5977	−0.5445	−0.2134	0.0264
18	8.0183	−0.5486	−0.2083	0.0252
19	6.3031	−0.5445	−0.2146	0.0267
20	4.9188	−0.5439	−0.2148	0.0270
21	9.3645	−0.5432	−0.2167	0.0271
22	7.9356	−0.5413	−0.2197	0.0279
23	3.6569	−0.5487	−0.2106	0.0256
24	5.1570	−0.5444	−0.2164	0.0271

and

$$\mathcal{N}_2 = \frac{X}{1+X}, \qquad (5)$$

where X is the ratio of the population of the upper level $N_2 \equiv N(^2P^o_{3/2})$ relative to the population of the lower level $N_1 \equiv N(^2P^o_{1/2})$. This ratio can be calculated from the relation:

$$X = \frac{N_2}{N_1} = \frac{N_{\rm e} C_{12}}{N_{\rm e} C_{21} + A_{21}}, \qquad (6)$$

where $A_{21} = 5.166\ 10^{-4}\ {\rm s^{-1}}$ is the magnetic dipole transition probability, calculated from the O^{3+} target wave functions described in Sect. 2, using the experimental energy difference. C_{12} is the excitation rate for the transition $^2P^o_{1/2} - ^2P^o_{3/2}$ and C_{21} is the de-excitation rate for this transition. The excitation rate can be expressed in form:

$$C_{12} = \frac{8.63\ 10^{-6}}{\omega(^2P^o_{1/2}) T_{\rm e}^{1/2}}\, \Upsilon_{12}\, \exp(-\Delta E/kT_{\rm e}), \qquad (7)$$

and the de-excitation rate is:

$$C_{21} = \frac{8.63\ 10^{-6}}{\omega(^2P^o_{3/2}) T_{\rm e}^{1/2}}\, \Upsilon_{12}, \qquad (8)$$

where the energy difference between the two lowest levels $P^o_{1/2}$ and $P^o_{3/2}$ of the recombining ion is $\Delta E = 0.0035166$ Ry, the electron temperature $T_{\rm e}$

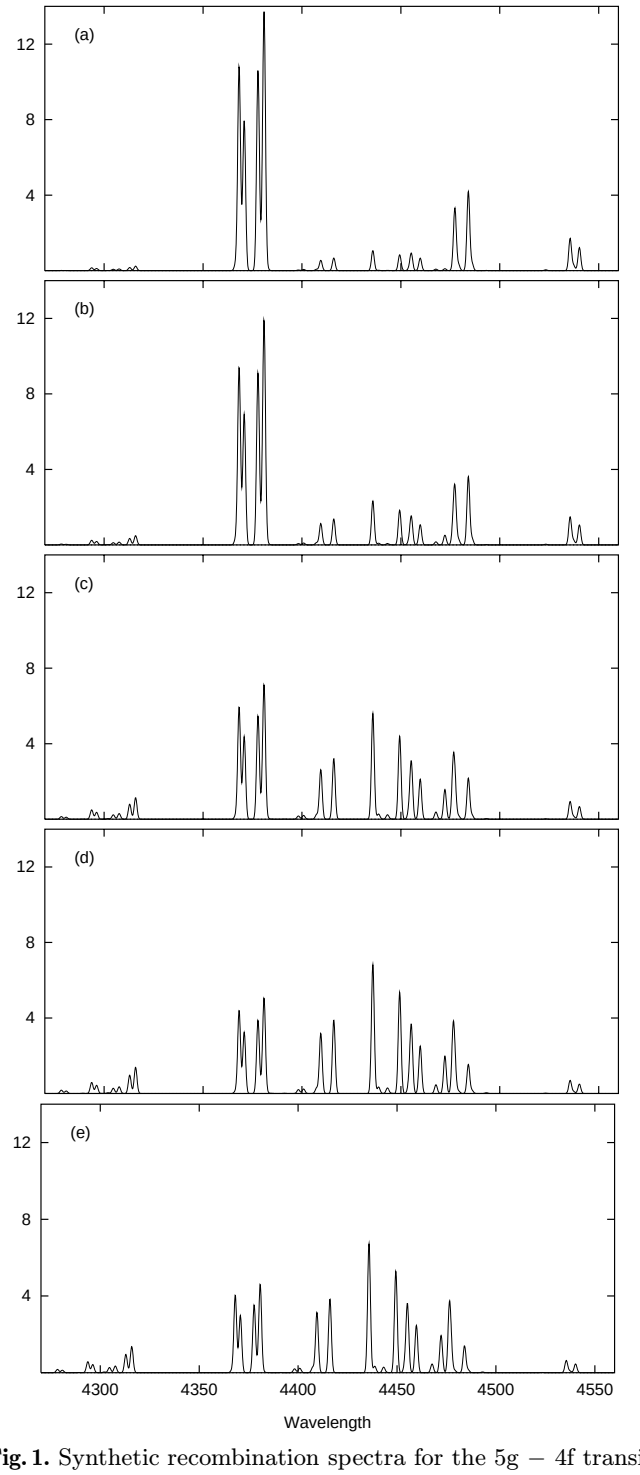

Fig. 1. Synthetic recombination spectra for the 5g − 4f transition array at electron temperature $T_e = 10\,000$ K and various electron densities: **a)** $N_e = 10^2$, **b)** $N_e = 10^3$, **c)** $N_e = 10^4$, **d)** $N_e = 10^5$, **e)** $N_e = 10^6$ cm^{-3}. The line profiles are Gaussian with $FWHM = 2\sqrt{\ln 2}$ Å

is expressed in K and the Boltzmann constant is $1/k = 1.57888\ 10^5$ [K Ry^{-1}].

The collision strengths Υ_{12} were taken from the R-matrix calculations of Blum & Pradhan (1992). These can be fitted to

Table 4. The fractions of the cascade contributions from each series to the recombination coefficients of the 5g levels of O $^{2+}$

n_1	$g_1^{casc}(J\pi)$	$g_2^{casc}(J\pi)$
13	0.85027	0.14973
14	0.85015	0.14985
15	0.96220	0.03780
16	0.96187	0.03813
17	0.03873	0.96127
18	0.03883	0.96117
19	0.06558	0.93442
20	0.06779	0.93221
21	0.03393	0.96607
22	0.03395	0.96605
23	0.00153	0.99847
24	0.00185	0.99814

$$\Upsilon_{12} = a_\Upsilon + b_\Upsilon \ln(t) + c_\Upsilon/t + d_\Upsilon/t^2, \quad (9)$$

where $t = T_e[\mathrm{K}]/10\,000$, $a_\Upsilon = 3.6292$, $b_\Upsilon = -0.5728$, $c_\Upsilon = -1.4231$ and $d_\Upsilon = 0.2101$. This fitting is valid for the temperature range $T_e = 4000 - 20\,000$ K, and the maximum fitting error is less than 0.25%.

Finally, the fractions $g_1^{casc}(J\pi)$ and $g_2^{casc}(J\pi)$ can be obtained from Table 4.

In order to calculate recombination coefficients for any 5g level of O $^{2+}$ at a specific electron temperature T_e and electron density N_e, one uses the expressions for the coefficients from Eqs. (1), (2) and (3), the data from Tables 3 and 4 and the recombining ion level population determined from Eqs. (4–9).

4. Results and discussion

In Table 5 we give recombination coefficients for the 5g $(J\pi)$ levels at temperatures of 10 000 K and 20 000 K, and a density of 10^3 cm^{-3}, calculated from Eq. (1) and from the fitting formulae given in Sect. 3.1. These are provided as a benchmark for the use of the formulae. The comparison shows that the fitted coefficients $\alpha_{\rm fit}$ agree with the calculated ones $\alpha_{\rm calc}$ within 1.5%. The intensities of any of the lines in the 5g − 4f transition array may be obtained, within the range of validity of the fits ($5000 \le T_e[\mathrm{K}] \le 20\,000$ K and $10^2 \le N_e[\mathrm{cm}^{-3}] \le 10^6$), by combining the recombination coefficients calculated from the formulae of Sect. 3.1 with the branching ratios in Table 2.

In Fig. 1 we show synthetic spectra of the entire 5g − 4f transition array calculated at $T_e = 10\,000$ K and various electron densities. The lines are taken to have a $FWHM$ of $2\sqrt{\ln 2}$ Å. Some of the lines show a pronounced variation in intensity with density at typical nebular densities, between 10^2 and 10^4 cm^{-3}. The line at 4434.6 Å, for example, which is the only transition from the $(^2\mathrm{P}^{\mathrm{o}}_{3/2})5\mathrm{g}\ ^3\mathrm{H}_6$ level (level 21 in Table 1) increases in intensity by a

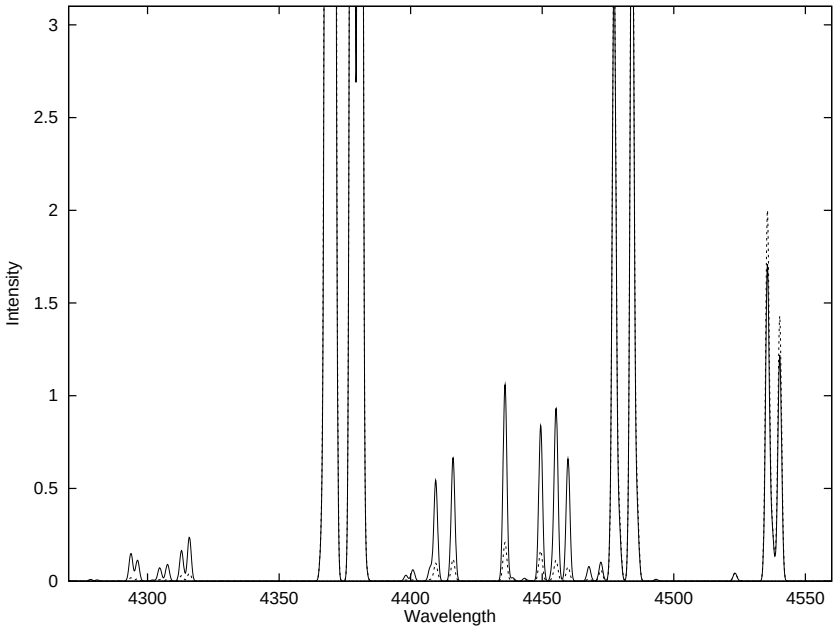

Fig. 2. Synthetic recombination spectra for the 5g − 4f transition array at electron temperature $T_e = 10\,000$ K and electron density $N_e = 10^2$ cm^{-3}. The dashed line shows the spectrum calculated using Eq. (10), the solid line using Eq. (1). The line profiles are Gaussian with $FWHM = 2\sqrt{\ln 2}$ Å

Table 5. Calculated $\alpha_{\rm calc}$ and fitted $\alpha_{\rm fit}$ effective recombination coefficients (in 10^{-12} cm^3 s^{-1}) for the 5g levels of O^{2+} at the electron temperatures $T_e = 10\,000$ K and $T_e = 20\,000$ K and the electron density $N_e = 10^3$ cm^{-3}. Indices n_1 correspond to the energy level indices from Table 1

	$T_e = 10\,000$ K		$T_e = 20\,000$ K	
n_1	$\alpha_{\rm calc}$	$\alpha_{\rm fit}$	$\alpha_{\rm calc}$	$\alpha_{\rm fit}$
13	1.130(−1)	1.122(−1)	5.263(−2)	5.195(−2)
14	8.785(−2)	8.722(−2)	4.093(−2)	4.039(−2)
15	1.262(−1)	1.253(−1)	5.893(−2)	5.816(−2)
16	1.542(−1)	1.530(−1)	7.200(−2)	7.106(−2)
17	1.662(−2)	1.652(−2)	6.647(−3)	6.574(−3)
18	2.033(−2)	2.021(−2)	8.130(−3)	8.041(−3)
19	1.979(−2)	1.966(−2)	8.153(−3)	8.060(−3)
20	1.560(−2)	1.550(−2)	6.443(−3)	6.369(−3)
21	2.315(−2)	2.301(−2)	9.188(−3)	9.087(−3)
22	1.961(−2)	1.949(−2)	7.781(−3)	7.696(−3)
23	6.749(−3)	6.712(−3)	2.507(−3)	2.482(−3)
24	9.523(−3)	9.472(−3)	3.542(−3)	3.506(−3)

factor of 5.3 between $N_e = 10^2$ and 10^4 cm^{-3} as the population of the O^{3+} ^{2}P$^o_{3/2}$ rises. The intensity of this line, which is one of the stronger lines in the 5g − 4f group, is 1.99 $N(O^{3+})/N(H^+)$ relative to H$_\beta$ at $T_e = 10\,000$ K and $N_e = 10^4$ cm^{-3}, where $N(O^{3+})$ and $N(H^+)$ are the number densities of O^{3+} and H$^+$ respectively.

The coefficients $g^{\rm casc}$ given in Table 4 show that the direct photorecombination and cascade contributions to each level are dominated by contributions from one or other of the O^{3+} parent states, ^{2}P$^o_{J_0}$, indicating that the 5g levels are approaching jj-coupling. We have investigated the effects of the interaction of the two series on the line intensities by carrying out a calculation of the coefficients in which there is no interaction. In this simpler approximation, we use hydrogenic recombination coefficients throughout. The recombination coefficients to the 5g $J\pi$ levels are directly proportional to the series parent population as follows:

$$\alpha\left[^2{\rm P}^{\rm o}_{J_0};\ 5{\rm g}\ (J\pi)\right] = \frac{N(^2{\rm P}^{\rm o}_{J_0})}{N(^2{\rm P}^{\rm o})}\ \alpha^{\rm eff}_{\rm H}(5{\rm g}) \times \frac{(2J+1)}{\omega(5{\rm g})\ (2J_0+1)}, \qquad (10)$$

where $\alpha_{\rm eff}(5{\rm g})$ is the total hydrogenic recombination coefficient to the 5g level (Storey & Hummer 1995) and J_0 is the total angular momentum of the parent level. This coefficient includes both the direct radiative recombination to the 5g level and the cascading processes from the higher levels.

To demonstrate the difference between the two approximations, we compare synthetic spectra for the two models in Fig. 2 at the lowest electron density, $N_e = 10^2$ cm^{-3}. At this density the fraction of the O^{3+} population in the ^{2}P$^o_{3/2}$ is very low (2%), so that in the approximation of Eq. (10), the Rydberg states (^{2}P$^o_{3/2}$)nl have very low populations and the resulting lines are weak, while in the more realistic approximation of Eq. (1), population can be transferred between the (^{2}P$^o_{1/2}$)nl and (^{2}P$^o_{3/2}$)nl series increasing the line intensities. It should be noted that the differences between the two approximations become smaller as the density increases and the parent state populations approach the Boltzmann distribution.

5. Conclusion

Effective recombination coefficients for the formation of O III lines in the 5g − 4f transition array have been calculated in the intermediate coupling scheme at temperatures and densities appropriate to nebular plasmas. The temperature and density dependence of the effective recombination coefficients has been factorized to permit the coefficients to be fitted. We have given formulae to enable the line effective recombination coefficients to be computed for any particular 5g level of O^{2+} as a function of electron temperature T_e and electron density N_e. Some of the lines of the 5g − 4f transition array are sensitive to the electron density of the emitting region, and might be suitable as a density diagnostic in objects where the abundance of O^{3+} is relatively large.

References

Berrington K.A., Burke P.G., Butler K., et al., 1987, J. Phys. B 20, 6379
Berrington K.A., Eissner W.B., Norrington P.N., 1995, Computer Phys. Commun. 92, 2459
Blum R.D., Pradhan A.K., 1992, ApJS 80, 425
Davey A.R., Storey P.J., Kisielius R., 1999, A&AS (in press)
Eissner W., Jones M., Nussbaumer H., 1974, Computer Phys. Commun. 15, 23
Escalante V., Victor G.A., 1990, ApJS 73, 513
Kisielius R., Storey P.J, Davey A.R, Neale L., 1998, A&AS 133, 257
Liu X.-W., Storey P.J., Barlow M.J., Clegg R.E.S., 1995, MNRAS 272, 369
Moore C.E., 1970, "Atomic Energy Levels", National Bureau of Standards, U.S.A.
Nussbaumer H., Storey P.J., 1978, A&A 64, 139
Péquignot D., Baluteau J.-P., 1994, A&A 283, 593
Péquignot D., Petitjean P., Boisson C., 1991, A&A 251, 680
Pettersson S.-G., 1982, Phys. Scr. 26, 296
Scott N.S., Taylor K.T., 1982, Computer Phys. Commun. 25, 347
Storey P.J., 1994, A&A 282, 999
Storey P.J., Hummer D.G., 1995, MNRAS 272, 41
Zeippen C.J., Seaton M.J., Morton D.C., 1977, MNRAS 181, 527